Vibration Mode Analysis of a 100m Simply-supported Steel Beam Bridge via POD of FEM

*A. J. Tikil [1], Y. Telue [2], S. Dunstan [3]

[1,3]School of Mathematics and Computer Science, Papua New Guinea University of Technology, Private Mail Bag, Lae, Morobe Province 411, Papua New Guinea

[2]Department of Civil Engineering, Lutheran University, P.O. Box 100, Lae, Morobe Province, Papua New Guinea

*Correspondence author email: japathtikil@gmail.com

Abstract: Bridge vibrations pose significant challenges to structural safety and longevity. This study employs the Finite Element Method (FEM) with Euler-Bernoulli beam elements and Proper Orthogonal Decomposition (POD) to analyze the dynamic response of a one-dimensional beam bridge model under sinusoidal external loading. The governing partial differential equation (PDE) describes the behavior of the lines with terms for inertial forces, damping, and flexural rigidity, discretized into a system of algebraic equations using finite elements of a 1D beam. This numerical approach simulates the bridge's linear displacement field over time and space, providing detailed understanding of its vibrational behavior through POD mode extraction. This study highlights the importance of integrating advanced computational tools, such as FEM and POD, into structural engineering practices. Furthermore, this research promotes the safe and sustainable development of infrastructure, particularly in the Pacific region, where rising sea levels and extreme weather events pose significant challenges.

Keywords: finite-element-method, Euler-Bernoulli, POD, bridge-infrastructure, Pacific-weather.

Presenter or Main Author Biography: Japath Tikil is a Master of Philosophy in Mathematics candidate at Papua New Guinea University of Technology, presenting for the first time at the PIURN Conference. His research applies computational methods (FEM and POD analysis) to study vibration patterns in 100-meter steel bridges, identifying dangerous movements caused by wind and traffic. By mapping a bridge's dominant swaying motions and weak points, his work helps engineers precisely place supports and dampers to prevent structural failures - offering practical safety solutions for Pacific Island infrastructure. Under the guidance of Professors Yaip Telue and Samuel Dunstan, Japath's research advances predictive maintenance for bridges through innovative vibration analysis

1. INTRODUCTION

Excessive bridge vibrations from periodic loads pose significant risks, as demonstrated by the 1940 collapse of the Tacoma Narrows Bridge, where wind-generated harmonic forces triggered a destructive resonance (Lin, Y 2022). Although that failure involved aerodynamic flutter, similar dynamics arise under distributed sinusoidal loading, the focus of this study. Here, we analyze a beam bridge subjected to the forcing function;

$$F(x,t) = \sin\left(\frac{\pi x}{L}\right) sin(2\pi f t) \quad (f = 1Hz)$$

The forcing function mimics rhythmic excitations (e.g., wind, machinery, or pedestrian loads).

The Proper Orthogonal Decomposition (POD), which is essentially the Singular Value Decomposition (SVD) algorithm applied to solutions of partial differential equations [Brunton, S. 2021], is employed here to extract dominant modes from the displacement field. By applying Finite Element Analysis (FEA) and the Finite

Element Method (FEM) to generate data and performing POD on the results, we quantify the displacement field $u(x,t)$ governed by the damped Euler-Bernoulli equation (Fryba, L., 1972; Wang, S., 2019) to assess resonance risks.

Advanced numerical methods, for which finite element methods are the most efficient frequently used, are extremely important for complicated engineering structures (Mackerle, J. 1999). The understanding and mitigation of these vibrations through FEA is critical to ensuring structural safety (Islam, A. 2014). This study combines these approaches to simulate bridge dynamics under sinusoidal loading and identify critical vibrational modes.

The problem is modeled using a partial differential equation (PDE) that describes the displacement of the bridge over time and space. The PDE accounts for inertial forces, damping, internal stiffness, and external forces. By discretizing the bridge into finite elements, the PDE is transformed into a system of algebraic equations, which are solved numerically. The results are further analyzed using POD to extract dominant vibrational patterns, providing a deeper understanding of the dynamic behavior of the bridge. The results are also compared with the spectral method for accuracy.

2. METHODOLOGY

The methodology involves discretizing the bridge, defining initial conditions, constructing mass and stiffness matrices, applying external forces, and solving the system using a time-stepping scheme. The results are then analyzed using POD to identify dominant vibrational modes.

3. GOVERNING PDE AND DISCRETIZATION

The vibrations of the bridge are governed by the equation of a damped one-dimensional beam with external forcing [3; 4]:

$$\rho\frac{\partial^2 u(x,t)}{\partial t^2} + c\frac{\partial u(x,t)}{\partial t} + EI\frac{\partial^4 u(x,t)}{\partial x^4} = F(x,t) \qquad (1)$$

where:

- $u(x,t)$ is the displacement (meters)
- ρ = 1.0 kg/m is the mass per unit length
- c = 0.01 N·s/m is the damping coefficient
- EI = 1.0 N·m^2 is the flexural rigidity
- $F(x,t) = \sin\left(\frac{\pi x}{L}\right) sin(2\pi f t)$ where f = 1 Hz is the external force (N/m)

The bridge of length L = 100 m is discretized using:

- FEM: n_{fem} = 128 points (equally spaced points distributed along the beam length from 0 to L with n_{fem} + 1 total grid points)

- Spectral: n_{spec} = 64 (Chebyshev-Gauss-Lobatto points distributed nonuniformly along the beam length [0, L], with higher point density near the boundaries, using n_{spec} + 1 discretization points)

4. INITIAL CONDITIONS

The initial conditions are:

$u_0(x) = \sin\left(\frac{\pi x}{L}\right)$ (Initial Displacement)

$v_0(x) = 0$ (Initial velocity)

5. STEP-BY-STEP DERIVATION OF THE EXACT SOLUTION (UNDAMPED, UNFORCED CASE)

For the undamped, unforced Euler-Bernoulli beam equation:

$$\rho \frac{\partial^2 u(x,t)}{\partial t^2} + EI \frac{\partial^4 u(x,t)}{\partial x^4} = 0$$

The clamped boundary conditions:

$$u(0,t) = u(L,t) = 0, \quad \frac{\partial y}{\partial x} = \frac{\partial u}{\partial x}(L,t) = 0$$

5.1 Step 1: Separation of Variables

Assume $u(x,t) = X(x)T(t)$Substituting into the PDE:

$$\rho X(x)T^{(2)}(t) + EIX^{(4)}(x)T(t) = 0$$

Divide by $X(x)T(t)$ yields two ODEs:

- Temporal ODE: $T^{(t)} + w^2 T(t) = 0$
- Spatial ODE: $X^{(4)}(x) - \frac{\rho\omega^2}{EI} X(x) = 0$

5.2 Step 2: Solve the Spatial ODE

Let $\beta^4 = \frac{\rho\omega^2}{EI}$. The spatial ODE becomes:

$$X^{(4)}(x) - \beta^4 X(x) = 0$$

General solution:

$$X(x) = A\cos(\beta x) + B\sin(\beta x) + C\cosh(\beta x) + D\sinh(\beta x)$$

Apply clamped boundary conditions at $x = 0$ and $x = L$ to determine β and mode shapes.
For the fundamental mode: Assume $X(x) = \sin\left(\frac{\pi x}{L}\right)$. Substituting into the ODE:

$$\left(\frac{\pi}{L}\right)^4 \sin\left(\frac{\pi x}{L}\right) - \beta^4 \sin\left(\frac{\pi x}{L}\right) = 0 \text{ Implies that } \beta = \frac{\pi}{L}$$

Natural frequency; $\omega = \sqrt{\frac{EI}{\rho}}\left(\frac{\pi}{L}\right)^2$

5.3 Step 3: Solve the Temporal ODE

Solution: $T(t) = E\cos(\omega t) + F\sin(\omega t)$

$$T(t) = E\cos(\omega t) + F\sin(\omega t)$$

For simplicity, assume $F = 0$

$$T(t) = \cos(\omega t)$$

5.4 Step 4: Combine Solutions

Exact solution:

$$u(x,t) = \sin\left(\frac{\pi x}{L}\right)\cos\left(\sqrt{\frac{EI}{\rho}}\left(\frac{\pi}{L}\right)^2 t\right).$$

5.5 Step 5: Verify Initial Conditions

At $t = 0$:

$$u(x,0) = \sin\left(\frac{\pi x}{L}\right).$$

6. ANALYTICAL SOLUTION OF ODE MODEL FOR TEMPORAL DYNAMICS

To complement the full beam solution and provide additional physical insight, we analyze a simplified damped harmonic oscillator model that captures the essential temporal dynamics:

$$\frac{d^2u}{dt^2} + 0.01\frac{du}{dt} + u = \sin(2\pi t)$$

where:

- $\frac{d^2u}{dt^2}$ is the acceleration
- $0.01\frac{du}{dt}$ represents viscous damping
- u is the displacement (spring restoring force)
- $\sin(2\pi t)$ is the harmonic driving force at 1 Hz

6.1 Solution Components

The complete solution consists of:

1. **Transient solution**: Natural response that decays exponentially
2. **Steady-state solution**: Persistent forced oscillation

6.2 Transient Solution

The homogeneous equation describes the system's natural behavior:

$$\frac{d^2u_h}{dt^2} + 0.01\frac{du_h}{dt} + u_h = 0$$

6.2.1 Characteristic Equation

Assuming solutions of form $u_h(t) = e^{rt}$ yields:

$$r^2 + 0.01r + 1 = 0$$

with roots: $r = -0.005 \pm \sqrt{1 - 2.5 \times 10^{-5}} \approx -0.005 \pm i$

6.2.2 General Form

The underdamped solution oscillates at the natural frequency while decaying:

$$u_h(t) = e^{-0.005t}(Acost + Bsint)$$

6.3 Steady-State Solution

For the particular solution with forcing $\sin(2\pi t)$

6.3.1 Assumed Form

$$u_p(t) = C\sin(2\pi t) + D\cos(2\pi t)$$

6.3.2 Coefficients

Substitution into the ODE gives:

$$(1 - 4\pi^2)C - 0.02\pi D = 1$$

$$0.02\pi C + (1 - 4\pi^2)D = 0$$

Yielding:

$$C \approx -0.0253, D \approx 1.69 \times 10^{-4} \approx -0.0253, \quad D \approx 1.69 \times 10^{-4}$$

6.3.3 Amplitude-Phase Representation

The solution can be expressed as:

$$u_p(t) = \frac{\sin(2\pi t - \phi)}{\sqrt{(1 - 4\pi^2)^2 + (0.02\pi)^2}} \approx 0.0253\sin(2\pi t + 0.0067)$$

where the phase shift $\phi \approx 0.0067\ radians$ $\phi \approx -0.0067$ radians.

6.4 Complete Solution

Combining components with zero initial conditions:

$$u(t) \approx 0.0253\sin(2\pi t + 0.0067)$$

This simplified model helps validate the temporal behavior observed in the full FEM solution, particularly the steady-state amplitude and phase characteristics.

7. FINITE ELEMENT METHOD FOR FORCED, DAMPED EULER-BERNOULLI BEAM

7.1 Shape Functions Definition

For a 2-node beam element of length h, the linear shape functions are:

$$N_1(x) = 1 - \frac{x}{h}, \quad N_2(x) = \frac{x}{h}$$

Node evaluations:

At $x = 0$: $N_1(0) = 1$, $N_2(0) = 0$
At $x = h$: $N_1(h) = 0$, $N_2(h) = 1$

7.2 Mass Matrix Formulation

Consistent mass matrix formulation

$$M_{local} = \rho \int_0^h \begin{bmatrix} N_1^2(x) & N_1(x)N_2(x) \\ N_1(x)N_2(x) & N_2^2(x) \end{bmatrix} dx$$

7.2.1 Term-by-Term Integration:

a) M_{11} **term:**

$$M_{11} = \rho \int_0^h \left(1 - \frac{x}{h}\right)^2 dx = \rho \int_0^h \left(1 - \frac{2x}{h} + \frac{x^2}{h^2}\right)^2 dx = \rho \left[x - \frac{x^2}{h} + \frac{x^3}{3h^2}\right]_0^h = \rho\left(h - h + \frac{h}{3}\right) = \rho\frac{h}{3}$$

b) M_{12} **term:**

c) $M_{12} = \rho \int_0^h \left(1 - \frac{x}{h}\right)\left(\frac{x}{h}\right) dx = \rho \int_0^h \left(\frac{x}{h} - \frac{x^2}{h^2}\right) dx = \rho \left[\frac{x^2}{2h} - \frac{x^3}{3h^2}\right]_0^h = \rho\left(\frac{h}{2} - \frac{h}{3}\right) = \rho\frac{h}{6}$

d) M_{22} **term:**

$$M_{22} = \int_0^h \left(\frac{x}{h}\right)^2 dx = \rho \left[\frac{x^3}{3h^2}\right]_0^h = \rho\frac{h}{3}$$

7.3 Final Assembly: $\boldsymbol{M_{local} = \frac{ph}{6}\begin{bmatrix} 2 & 1 \\ 1 & 2 \end{bmatrix}}$

Numerical example (ρ = 1.0kg/m, h = 0.78125m):

$$\boldsymbol{M_{local} = \frac{1\frac{kg}{m} \times 0.78125m}{6}\begin{bmatrix} 2 & 1 \\ 1 & 2 \end{bmatrix}}$$
$$\boldsymbol{= \begin{bmatrix} 0.2604 & 0.1302 \\ 0.1302 & 0.204 \end{bmatrix} kg}$$

7.4 Beam Bending Formulation

7.4.1 Weak Form $\boldsymbol{\int_0^h EI}$

$$\int_0^h EI \frac{d^2}{dx^2}\frac{d^2v}{dx^2} dx = \int_0^h q(x)\, v(x) dx$$

7.4.2 Cubic Hermite Shape Functions:

$$H_1(x) = 1 - 3\left(\frac{x}{h}\right)^2 + 23\left(\frac{x}{h}\right)^3$$

$$H_2(x) = x\left(1 - \frac{x}{h}\right)^2$$

$$H_3(x) = 3\left(\frac{x}{h}\right)^2 - 2\left(\frac{x}{h}\right)^3$$

$$H_4(x) = \frac{x^2}{h}\left(\frac{x}{h} - 1\right)$$

7.4.3 Full Stiffness Matrix:

$$K_{full} = \frac{EI}{h^3}\begin{bmatrix} 12 & 6h & -12 & 6h \\ 6h & 4h^2 & -6h & 2h^2 \\ -12 & -6h & 12 & -6h \\ 6h & 2h^2 & -6h & 4h^2 \end{bmatrix}$$

7.5 Static Condensation

7.5.1 Step 1: Partitioning

$$\boldsymbol{K}_{full} = \begin{bmatrix} \boldsymbol{K}_{\omega\omega} & \boldsymbol{K}_{\omega\theta} \\ \boldsymbol{K}_{\theta\omega} & \boldsymbol{K}_{\theta\theta} \end{bmatrix}$$

Where:

$$\boldsymbol{K}_{\omega\omega} = \frac{EI}{h^3}\begin{bmatrix} 12 & -12 \\ -12 & 12 \end{bmatrix}, \boldsymbol{K}_{\omega\theta} = \frac{EI}{h^3}\begin{bmatrix} 6h & 6h \\ -6h & -6h \end{bmatrix}, \boldsymbol{K}_{\theta\theta} = \frac{EI}{h^3}\begin{bmatrix} 4h^2 & 2h^2 \\ 2h^2 & 4h^2 \end{bmatrix}$$

7.5.2 Step 2: Inversion

$$K_{\theta\theta}^{-1} = \frac{1}{12h^4}\begin{bmatrix} 4h^2 & -2h^2 \\ -2h^2 & 4h^2 \end{bmatrix} = \frac{1}{3h^2}\begin{bmatrix} 1 & -\frac{1}{2} \\ -\frac{1}{2} & 1 \end{bmatrix}$$

7.5.3 Step 3: Multiplication

$$K_{\omega\theta}K_{\theta\theta}^{-1} = \frac{EI}{h^4}\begin{bmatrix} 1 & -1 \\ 1 & -1 \end{bmatrix}\mathbf{A}$$

$$AK_{\theta\omega} = \frac{EI}{h^3}\begin{bmatrix} 12 & -12 \\ -12 & 12 \end{bmatrix}$$

$$K_{\theta\omega} = \frac{EI}{h^3}\begin{bmatrix} 1 & -2 & 1 \\ -2 & 4 & -2 \\ 1 & -2 & 1 \end{bmatrix}\mathbf{AK}$$

7.5.4 Step 4: Condensation $\boldsymbol{K_{condensed} = K_{\omega\omega} - AK}$

7.6 System Matrices

7.6.1 Stiffness Matrix Assembly:

$$K_{fem} = [i-1:i+2, i-1:i+2] += \frac{EI}{h^3}\begin{bmatrix} 1 & -2 & 1 \\ -2 & 4 & -2 \\ 1 & -2 & 1 \end{bmatrix}$$

7.6.2 Damping Matrix:

$\mathbf{C}\text{fem} = \alpha\mathbf{M}\text{fem} + \beta\mathbf{K}\text{fem}$ or $c\mathbf{M}\text{fem}$

7.7 Boundary Conditions

7.7.1 Clamped ends implementation:

Left End:

$\mathbf{M}_{\text{fem}}[0,:] = \mathbf{0}$, $\mathbf{M}_{\text{fem}}[0,0] = 1$
$\mathbf{K}_{\text{fem}}[0,:] = \mathbf{0}$, $\mathbf{K}_{\text{fem}}[0,0] = 1$
$\mathbf{C}_{\text{fem}}[0,:] = \mathbf{0}$, $\mathbf{C}_{\text{fem}}[0,0] = 1$

Right End:

$\mathbf{M}_{\text{fem}}[-1,:] = \mathbf{0}$, $\mathbf{M}_{\text{fem}}[-1,-1] = 1$
$\mathbf{K}_{\text{fem}}[-1,:] = \mathbf{0}$, $\mathbf{K}_{\text{fem}}[-1,-1] = 1$ $\mathbf{C}_{\text{fem}}[-1,:] = \mathbf{0}$, $\mathbf{C}_{\text{fem}}[-1,-1] = 1$

7.8 Time Integration (Crank-Nicolson) A

$$A = M + \frac{\Delta t}{2}\left(C + \frac{\Delta t}{2}K\right)$$

$$\boldsymbol{b} = \left(M - \frac{\Delta t}{2}\left(C + \frac{\Delta t}{2}K\right)\right)V_{prev} + \Delta t\boldsymbol{F}(t)$$

Solve for v_{next}; $V_{next} = A^{-1}b$

Update the displacement: $u_{next} = u_{prev} + \Delta t v_{next}$

8. THE SPECTRAL METHOD IS APPLIED AS A NUMERICAL METHOD TO FIND SOLUTION OF THE FORCED, DAMPED EULER-BERNOULLI EQUATION (F(X, T) AND C ARE NOT EQUAL TO ZERO) TO VERIFY THE RESULTS OBTAINED IN FEM

8.1 Discretization Using Chebyshev Points

The first step in the spectral method is selecting an appropriate grid (discretization points). Unlike uniform grids (used in finite differences), spectral methods often use Chebyshev-Gauss-Lobatto (CGL) points, which are clustered near the boundaries (ends of the domain). This clustering helps in resolving boundary layers and improves accuracy. For a beam of length L = 100 m, we define N = 64 Chebyshev points as:

$$x_j = \frac{L}{2}\left(1 - \cos\left(\frac{j\pi}{N}\right)\right), j = 0,1,\ldots,N$$

These points are non-uniform, with higher density near x = 0 and x = L. The clustering helps in accurately capturing boundary effects (since beam vibrations are strongly influenced by clamped/fixed ends).

8.2 Chebyshev Differentiation Matrices

Since the beam equation involves a fourth derivative $\frac{\partial^4 u}{\partial x^4}$, we need a way to compute derivatives numerically at the Chebyshev points. This is done using Chebyshev differentiation matrices.

8.2.1 First Derivative Matrix ($\mathbf{D}_1$)

The first derivative of a function $u(x)$ at the Chebyshev points can be approximated as:

$$\frac{du}{dx} \approx \boldsymbol{D_1 u}\mathbf{u}$$

where $\mathbf{D}_1$ is an $(N+1) \times (N+1)$ matrix with entries:

$$(D_1)_{ij} = \begin{cases} \dfrac{c_i(-1)^{i+j}}{c_j(x_i - x_j)}, & if\ i \neq j \\ -\sum_{k \neq i} (D_1)_{ik}, & if\ i = j \end{cases}$$

where:

- $c_i = 2$ if $i = 0$ or $i = N$ (endpoints)
- $c_i = 1$ otherwise

8.2.2 Higher-Order Derivatives ($\mathbf{D}_2$, $\mathbf{D}_3$, $\mathbf{D}_4$)

The second, third, and fourth derivative matrices are obtained by matrix powers:

$$\mathbf{D}2 = (\mathbf{D}1)2, \qquad \mathbf{D}3 = (\mathbf{D}1)3, \qquad \mathbf{D}4 = (\mathbf{D}1)4$$

This means that the fourth derivative $\frac{\partial^4 u}{\partial x^2}$ is approximated as $\mathbf{D}_4 \cdot \mathbf{u}$.

8.3 Applying Boundary Conditions (Clamped Beam)

The beam has clamped boundary conditions at both ends:

$$u(0,t) = u(L,t) \qquad (Zero\ displacements)$$

$$\frac{\partial u}{\partial x}(0,t) = \frac{\partial u}{\partial x}(0,t) = 0 \qquad (zero\ slope)$$

8.3.1 Modifying the Differentiation Matrix

To enforce these conditions:

1. We remove the first and last two rows and columns of $\mathbf{D}_4$ (since they correspond to the boundary points)
2. The modified matrix $\mathbf{K}_{spec} = EI \cdot \mathbf{D}_4[2: -2, 2: -2]$ now represents the stiffness operator for the interior points

8.4 Solving the Dynamic Beam Equation

The full PDE for the beam is:

$$\rho \frac{\partial^2 u(x,t)}{\partial t^2} + c \frac{\partial u(x,t)}{\partial t} + EI \frac{\partial^4 u(x,t)}{\partial x^4} = F(x,t)$$

8.4.1 Time Discretization (Using Finite Differences)

We use the Crank-Nicolson method (an implicit time-stepping scheme) for stability:

1. Discretize time as $t_n = n\Delta t$
2. Approximate derivatives as:

$$\frac{\partial^2 u}{\partial t^2} \approx \frac{u^{n+1} - 2u^n + u^{n-1}}{\Delta t^2}$$
$$\frac{\partial u}{\partial t} \approx \frac{u^{n+1} - u^{n-1}}{2\Delta t}$$

3. The resulting system is: $I\left(\frac{\rho}{\Delta t^2} + c\frac{\rho}{2\Delta t} + EIK_{spec}\right)u^{(n+1)} = F^{(n+1)} + \left(2\rho\frac{I}{\Delta t^2} - c\frac{I}{2\Delta t}\right)u^{(n-1)}$

This is a linear system solved at each time step

9 SUMMARIES OF FINITE ELEMENT METHOD AND SPECTRAL METHOD FOR DYNAMIC BEAM RESPONSE

9.1 Finite Element Method (FEM)

The dynamic response of the beam is governed by the partial differential equation:

$$\rho \frac{\partial^2 u(x,t)}{\partial t^2} + c \frac{\partial u(x,t)}{\partial t} + EI \frac{\partial^4 u(x,t)}{\partial x^4} = F(x,t) \quad (2)$$

where:

- $u(x,t)$ is the transverse displacement
- ρ is the mass per unit length (kg/m)
- c is the viscous damping coefficient (N·s/m)
- EI is the flexural rigidity (N·m^2)
- $F(x,t)$ is the distributed external force (N/m)

The finite element solution is obtained by solving the discrete system:

$$\mathbf{M}\mathbf{u}''(t) + \mathbf{C}\mathbf{u}'(t) + \mathbf{K}\mathbf{u}(t) = \mathbf{F}(t) \quad (3)$$

where:

- $\mathbf{M}$ is the global mass matrix
- $\mathbf{C}$ is the global damping matrix ($\mathbf{C} = \alpha\mathbf{M} + \beta\mathbf{K}$ for Rayleigh damping)
- $\mathbf{K}$ is the global stiffness matrix
- $\mathbf{F}(t)$ is the nodal force vector
- $\mathbf{u}(t)$, $\mathbf{u}'(t)$, and $\mathbf{u}''(t)$ are the displacement, velocity, and acceleration vectors respectively

9.1.1 FEM Implementation Steps

1. **Matrix Construction:**

- Derive element mass matrix using shape functions:

$$\boldsymbol{M_e} = \rho \int_0^h \boldsymbol{N^T N}\, dx\mathbf{M}$$

- Derive element stiffness matrix:

$$\boldsymbol{K_e} = \boldsymbol{EI} \int_0^{\boldsymbol{h}} \boldsymbol{B^T B dx}\mathbf{K}$$

where $B = d^2\mathbf{N}/dx^2$

2. **Time Integration:**

- Apply Crank-Nicolson scheme:

$$\left(M + \frac{\Delta t}{2}C + \frac{\Delta t^2}{4}K\right)u_{n+1} = \left(M - \frac{\Delta t}{2}C - \frac{(\Delta t)^2}{4}K\right)u_n + \frac{\Delta t}{2}(F_n + F_{n+1})$$

3. **Boundary Conditions:**

- For clamped ends ($x = 0, L$):

$$u = 0 \text{ and } \frac{\partial u}{\partial x} = 0$$

implemented by modifying system matrices:

$\mathbf{K}_{ii} = 1, \qquad \mathbf{K}_{ij} = \mathbf{K}_{ji} = 0 \qquad$ for constrained DOFs

9.1.2 Connection between Continuous and Discrete Forms

The discrete system (2) exactly corresponds to the continuous PDE (1) through:

- $\mathbf{M}\ddot{\mathbf{u}}$ discretizes $\rho \frac{\partial^2 u}{\partial t^2}$
- $\mathbf{C}\dot{\mathbf{u}}$ discretizes $\rho \frac{\partial u}{\partial t}$
- $\mathbf{Ku}$ discretizes $EI \frac{\partial^4 u}{\partial x^4}$
- $\mathbf{F}(t)$ represents the projection of $F(x,t)$ onto nodal forces

9.2 Spectral Method Validation

The spectral method is used to validate the results obtained from the Finite Element Method by providing a high-accuracy solution for the beam's displacement. The spectral method involves solving the beam equation using Chebyshev differentiation for the fourth derivative of the displacement function. The steps in the Spectral Method are as follows:

- Discretization: The beam is discretized into a grid of points, and the fourth derivative operator $\mathbf{D}_4$ is approximated using Chebyshev differentiation. • Boundary Conditions: Clamped boundary conditions are incorporated by modifying the stiffness matrix and removing the first and last points in the grid.

- Solution: The displacement $\mathbf{u}(x,t)$ is computed by solving the system of equations derived from the spectral method using the time-dependent forcing function.
  The displacement $\mathbf{u}(x,t)$ from the spectral method is obtained by solving the matrix equation:

$$\mathbf{K}_{\text{spec}}\mathbf{u}(x,t) = \mathbf{F}(x,t)$$

where $\mathbf{K}_{\text{spec}}$ is the stiffness matrix obtained from the spectral method, and $\mathbf{F}(x,t)$ is the external force. The results from the spectral method are then compared with the results from the FEM to validate the accuracy of the numerical solution.

9.3 Validation and Comparison

The displacement **u**(*x,t*) obtained from the FEM is validated by comparing it with the displacement obtained from the spectral method. The agreement between the two methods serves as a verification of the FEM implementation. If the results from both methods show close agreement, it confirms that the FEM is correctly capturing the dynamic behavior of the beam.
The spectral method provides a more accurate solution for comparison due to its high-order accuracy, and thus, serves as a benchmark for validating the FEM results.

10 PROPER ORTHOGONAL DECOMPOSITION

Performed on centered FEM data:

10.1 Mean Displacement

The mean displacement is calculated as:

$$\bar{u}(x) = \frac{1}{N}\sum_{i=1}^{N} u(x, t_i)$$

where N is the total number of time steps, and $u(x,t_i)$ is the displacement at position x and time t_i.

10.2 Snapshot Matrix

The snapshot matrix **U** is constructed with the displacement values at each spatial location x and time step t_i, as follows:

$$U = \begin{bmatrix} u(x_1, t_1) & \dots & u(x_1, t_N) \\ \vdots & \ddots & \vdots \\ u(x_m, t_1) & \cdots & u(x_m, t_N) \end{bmatrix}$$

where:

- m is the number of spatial points.
- N is the number of time steps.
- $u(x_i,t_j)$ represents the displacement at the spatial point x_i and time step t_j.

Proper Orthogonal Decomposition is performed on centered FEM data:

$$mean\ displacement = \frac{1}{N}\sum_{i=1}^{N} u(x_i, t_j)$$

Centered data = $\mathbf{u}(x_i,t_j)$ − mean

SVD: $\mathbf{U\Sigma V}^T$ = centered data [2]

11 THE VALIDATION RESULTS TO VALIDATE THE FINITE ELEMENT METHOD

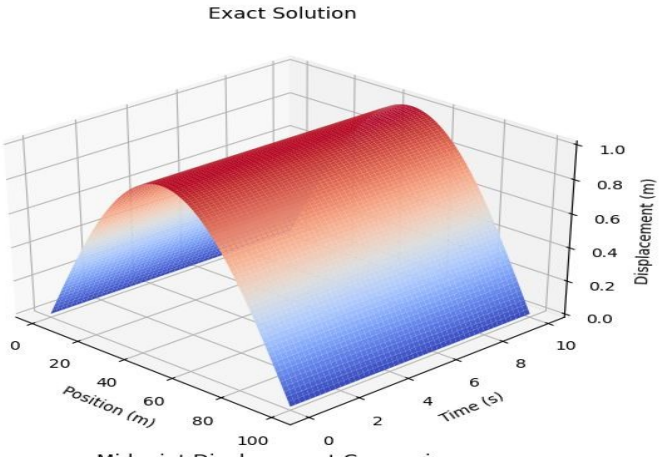

Figure 1: The exact solution for c=0 and F(x,t)=0

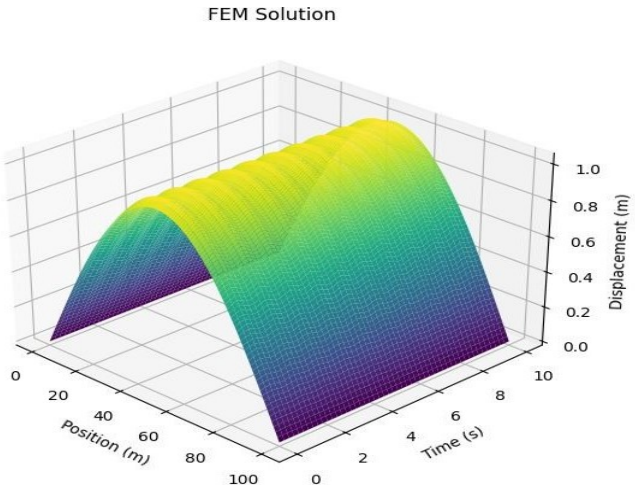

Figure 2: FEM solution with $c = 0$ and $F(x,t) = 0$

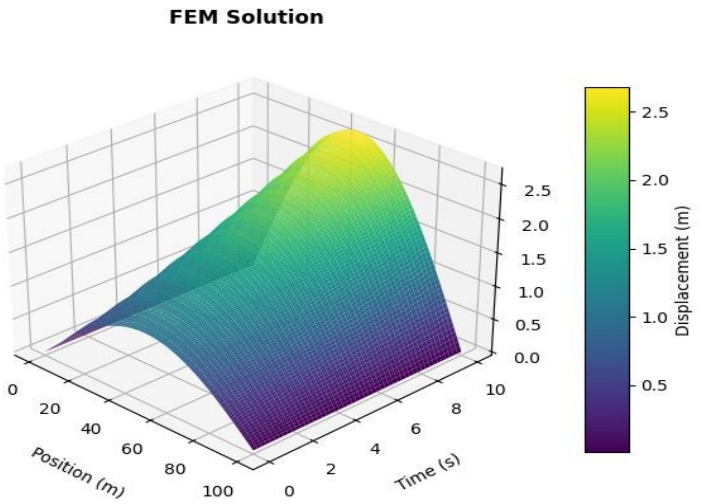

Figure 3: The full FEM solution with both c and $F(x,t)$ not equal to zero

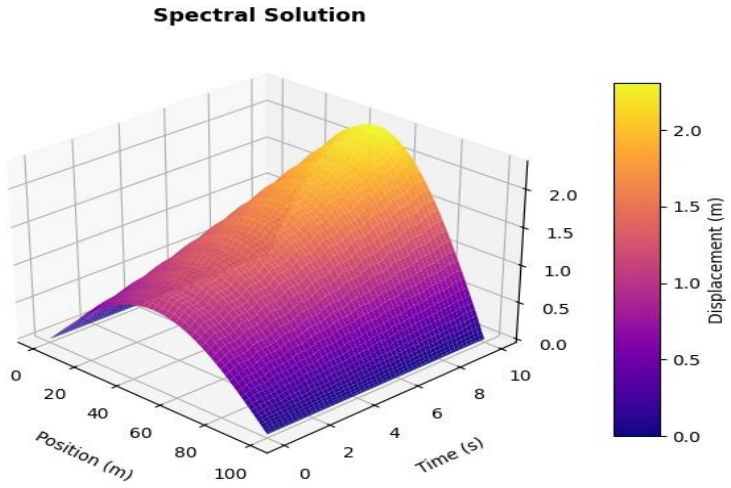

Figure 4: The full spectral solution with both c and $F(x,t)$ not equal to zero

11.1 The discussion of the validation results to validate the Finite Element Method

The PDE:

$$\rho\frac{\partial^2 u(x,t)}{\partial t^2} + c\frac{\partial u(x,t)}{\partial t} + EI\frac{\partial^4 u(x,t)}{\partial x^4} = F(x,t)$$

does not have an exact solution when $F(x,t)$ is not equal to zero and c is not equal to zero, so the spectral solution as shown in Figure 4 is compared to the Finite Element Method solution as shown in Figure 5 and the results are identical which validates the FEM.

More validation of the Finite Element Method is done by equating $F(x,t)$ and the damping coefficient c to zero and the results shown in Figure 2 and Figure 1 are identical, which then validates the FEM.

12 RESULTS

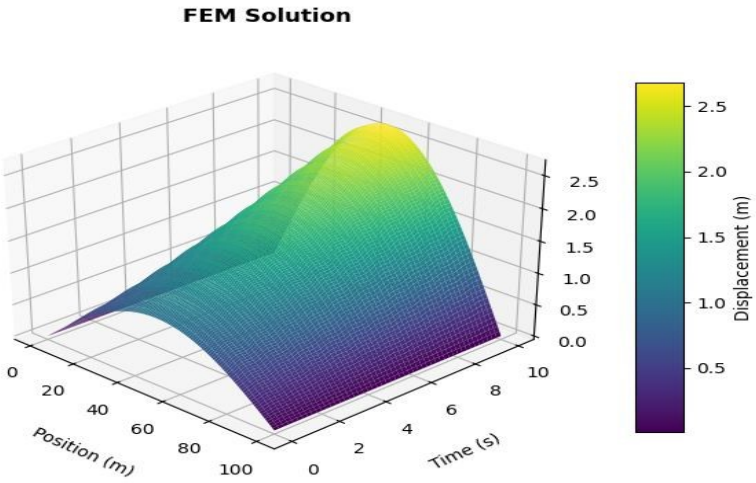

Figure 5: The full FEM solution with both c and $F(x,t)$ not equal to zero

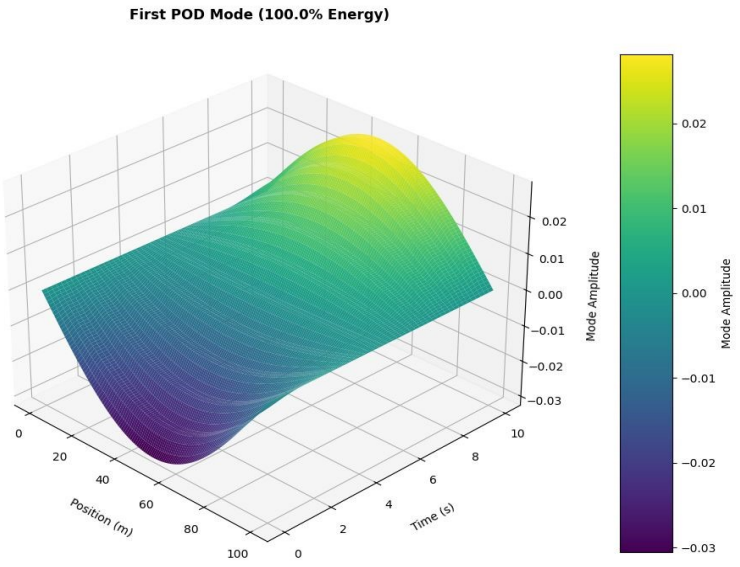

Figure 6: First dominant POD mode from the FEM data capturing the foundational vibrational mode of the bridge with lowest frequency and peak displacements

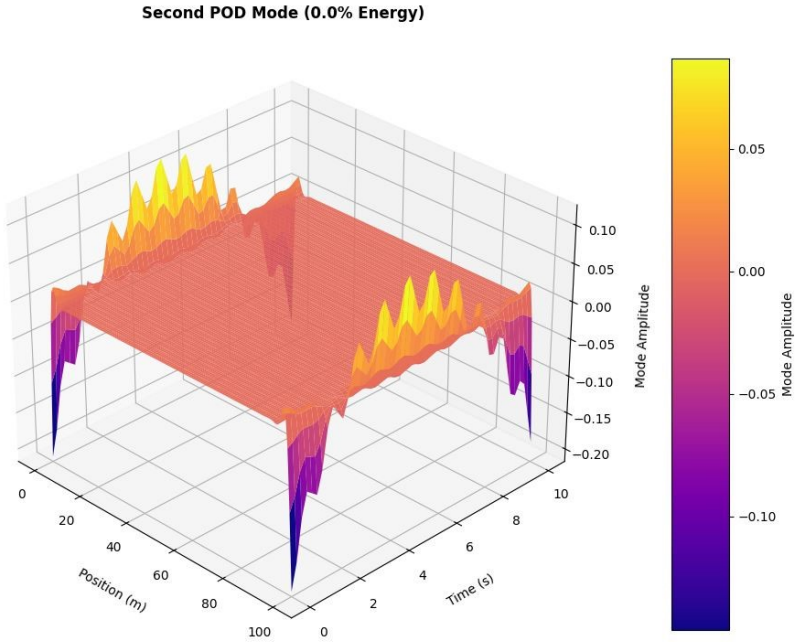

Figure 7: Second dominant POD mode from the FEM data capturing the next significant vibrational pattern with higher natural frequencies and larger local displacements.

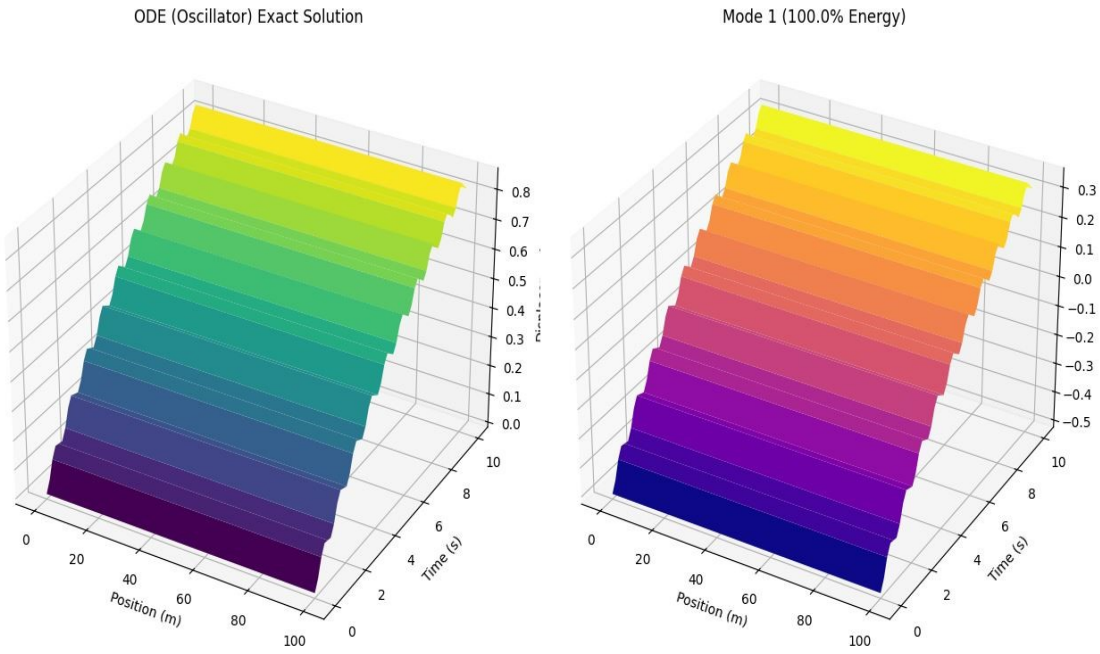

Figure 8: The 3D graph on the left shows the plot of the exact solution of the ODE: $u(t) \approx 0.0253\sin(2\pi t + 0.0067)$ and the graph on the right shows the Single dominant POD mode

13 DISCUSSIONS

13.1 FEM Full Solution Result

The full solution of the system obtained using the Finite Element Method (FEM) provides a comprehensive understanding of the vibrational behavior of the bridge over time. As shown in Figure 5, the three-dimensional plot illustrates the evolution of displacement along the length of the bridge. The peaks in the plot correspond to areas of maximum displacement, which are critical for identifying regions susceptible to structural stress. The sinusoidal nature of the external force is reflected in the periodic oscillations observed in the solution. This result confirms that the bridge experiences significant vibrations, particularly at specific points along its length, which could lead to fatigue or failure if not properly addressed.

13.2 First POD Mode Result

The first Proper Orthogonal Decomposition (POD) mode, as depicted in Figure 6, represents the most dominant vibrational pattern of the bridge. This mode captures the long-wavelength oscillation, which is characterized by a smooth sinusoidal deformation throughout the length of the bridge. The first mode accounts for the largest portion of the system's energy, as indicated by the corresponding singular value. This result is particularly useful for engineers because it highlights the primary mode of vibration that contributes most significantly to the dynamic response of the bridge.

13.3 Second POD Mode Result

The second POD mode, shown in Figure 7, represents a higher frequency vibrational pattern with more localized oscillations. Unlike the first mode, which spans the entire bridge, the second mode exhibits shorter wavelengths and more concentrated areas of displacement. This mode is crucial for identifying secondary vibrational behaviors that may not be as immediately apparent in the full FEM solution. The significance of the second mode lies in its ability to reveal potential stress concentrations or localized weaknesses in the structure of the bridge. Engineers can use this information to implement localized reinforcements or to design specific damping strategies that address these higher frequency vibrations, further improving the bridge's resilience to dynamic loads.

13.4 Engineering Insight and Practical Applications

The combination of the FEM full solution and the POD modes provide a powerful framework for analyzing and addressing bridge vibrations. The FEM solution offers a detailed, time-dependent view of the bridge's response to external forces, while the POD modes distill this information into dominant patterns that are easier to interpret and act upon. By understanding the first and second POD modes, engineers can prioritize design modifications that target the most critical vibrational behaviors.

13.5 Ordinary Differential Equation vs. Partial Differential Equation Comparison

The 3D graph in Figure 8 (left) shows the plot of the exact solution; $u \approx 0.0253\sin(2\pi t + 0.007)$of the ODE $\frac{\partial^2 u}{dt^2} + 0.01\frac{du}{dt} + u = \sin(2\pi)$ solution governed by:

$$\frac{\partial^2 u}{dt^2} + 0.01\frac{du}{dt} + u = \sin(2\pi)\ where\ u \approx 0.0253\sin(2\pi t + 0.007)$$

The equation represents a **damped harmonic oscillator** where $\frac{d^2u}{dt^2}$ is the **inertia term** (acceleration) $0.01\frac{du}{dt}$ is the **damping term** (friction), *u* is the **restoring force** (spring-like force), and sin(2*πt*) is the **driving term** (external periodic forcing).

The 3D graph in Figure 8 (right) shows the single dominant POD Mode 1 which captures 100% energy. The ODE exhibits one temporal mode that is identical to the exact solution, with no Mode 2 or Mode 3 contributing any energy at all. When comparing it with the POD modes of the Euler-Bernoulli PDE:

$$\rho\frac{\partial^2 u(x,t)}{\partial t^2} + c\frac{\partial u(x,t)}{\partial t} + EI\frac{\partial^4 u(x,t)}{\partial x^4} = F(x,t)$$

where ρ = 1.0 kg/m, c = 0.01 N·s/m is the damping coefficient, EI = 1.0 N·m^2 is the flexural rigidity and $F(x,t) = \sin\left(\frac{\pi x}{L}\right) sin(2\pi f t)$ is the external force (N/m), it shows multiple spatial modes, where Mode 1 is not equal to Mode 2, and neither mode matches the exact FEM solution, resulting in energy being distributed across the modes.

14 CONCLUSION

This study presents an integrated FEM-POD methodology for vibration analysis of a 100m steel beam bridge under harmonic loading. The computational approach successfully identified two dominant vibration modes: a global bending pattern governing the overall structural response and localized oscillations revealing critical stress concentrations. The results demonstrate that harmonic excitation induces characteristic vibration patterns that can be systematically analyzed using this framework. The

developed methodology offers an effective tool for vibration assessment in bridge engineering, with applications extending to similar slender structures subjected to periodic dynamic loads.

15 ACKNOWLEDGEMENTS

The first acknowledgment goes to the principal supervisor Dr Samuel Dunstan for his continuous guidance and support in writing this paper. The second acknowledgement extends to Professor Y. Telue for his professional and technical advice in writing the paper.

REFERENCES

Lin, Y., Zhang, Q., Chen, W.**:** Research on the collapse of Tacoma narrows bridge under the finite element application ANSYS of computational mechanics. Journal of Physics: Conference Series 2230, 012018 (2022).

Brunton, S. L., Kutz, J. N.: Data-driven science and engineering: Machine learning, dynamical systems, and control. 2nd edn. Cambridge University Press (2021).

Wang, S., Zhao, W., Zhang, G., Li, F., Du, Y.: Fourier series approach for the vibration of Euler-Bernoulli beam under moving distributed force: Application to train gust. Shock and Vibration 2019, 2175841 (2019).

Fryba, L.: Vibration of solids and structures under moving loads. Noordhoff International Publishing (1972).

Mackerle, J.: Finite element vibration and dynamic response analysis of engineering structures: A bibliography (1994–1998). Finite Elements in Analysis and Design 32(3), 179–192 (1999).

Islam, A. K. M. A., Li, F., Hamid, H., Jaroo, A.: Bridge condition assessment and load rating using dynamic response. Report No. 134695. Youngstown State University (2014).